NANO LETTERS

pubs.acs.org/NanoLett Letter

Folding Graphene into a Chern Insulator with Light Irradiation

Gan Zhao, Haimen Mu, Feng Liu, and Zhengfei Wang*

Cite This: *Nano Lett.* 2020, 20, 5860−5865 Read Online

ACCESS | Metrics & More | Article Recommendations | Supporting Information

ABSTRACT: Recently, the precise folding of flexible graphene is reported experimentally [*Science*, 2019, *365*, 1036−1040], demonstrating an efficient approach to manipulate its electronic and optoelectronic properties. Here, we propose a light-induced high-Chern-number Chern insulator (CI) in the folded graphene. Along both armchair and zigzag folding directions, we demonstrate that there are two-handedness-dependent chiral interface states localized at the curved region. Physically, they can be attributed to the light-induced mass-term inversion across the folded graphene. Most remarkably, by rationally designing the folding processes, 2D and 3D CIs are also realizable in a single-wall carbon nanotube and periodic folded graphene, respectively, illustrating a high tunability of the folding degree of freedom. We envision that this intriguing form of "foldtronics" will provide a new platform for investigating the topological state in 2D materials to draw immediate experimental attention.

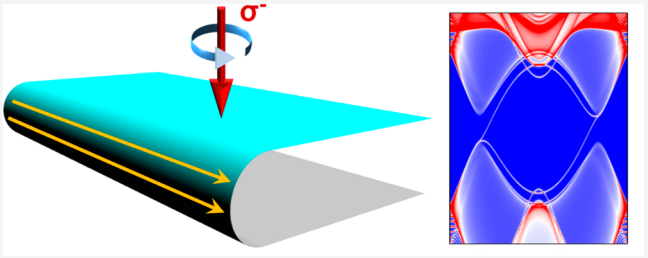

KEYWORDS: *foldtronics, graphene, nanotube, chiral interface state, Chern insulator*

The prosperity of a modern society is largely driven by the rapid development of semiconductor science and technology, where the information is stored and transmitted by different carriers in solid-state materials. From the original electronics to the latest spintronics and valleytronics, charge, spin, and valley degrees of freedom of electrons[1−3] have been harnessed to greatly enrich the designing strategy for the next-generation quantum devices. Very recently, Gao et al. reported that monolayer graphene could be precisely folded and unfolded along custom-designed directions by a scanning tunneling microscope (STM) tip,[4] paving a tunable way for artificially constructing the twisted bilayer graphene[5−8] with different twist angles and the tubular-edged bilayer graphene[9−11] with different chirality. Taking advantage of this technical breakthrough, we demonstrate a new principle to manipulate electronic and optoelectronic properties of 2D materials[12] via the folding degrees of freedom, which we coined as foldtronics.

Based on the floquet band theory, a variety of light-induced topological states have been reported.[13−23] These short-lived nontrivial states constitute a unique class of topological material, which is useful for investigating time-dependent topological physics and designing ultrafast optoelectronic devices. As a simple model system, graphene has been used to study Dirac-band associated topological phases.[24−27] Theoretically, the light-irradiated graphene can open a nontrivial gap at the Dirac point, transiting it from a semimetal to a Chern insulator (CI),[13,28] to exhibit the quantum anomalous Hall effect. Recently, driven by the femtosecond pulse of circularly polarized light (CPL), a nearly quantized anomalous Hall conductance was observed experimentally in graphene,[29] confirming this long-waiting prediction while demonstrating the possibility to detect an ultrafast transport signal of floquet topological states.

In this Letter, we propose a highly tunable strategy to manipulate the light-induced chiral interface states (chiral-ISs) in the folded graphene. Utilizing one CPL, the high-Chern-number (high-C) and 3D CIs are realized in single folded and periodic folded graphene, respectively. Moreover, at the limit of seamlessly folded graphene, the high-C CI in a single-wall carbon nanotube (SWCNT) is also presented. Our results demonstrate a high degree of tunability of the folding degree of freedom to control the topological interface states in 2D materials, paving a new way of designing foldtronic topological devices in the future.

Due to the bulk-boundary correspondence,[30] generally, the topological boundary state exists at two different types of interface. For the type-I interface, it is between a nontrivial phase and a vacuum, such as the topological insulator materials that support the topological surface or edge state.[30−32] For the type-II interface, it is between two nontrivial phases with opposite mass terms, such as the topological valley materials that support the topological interface state.[33−35] Different from the natural atomic boundary for the type-I interface, which has been widely studied, so far, it remains a challenging task to

Received: April 24, 2020
Revised: July 11, 2020
Published: July 13, 2020

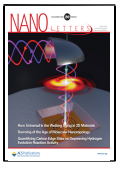

https://dx.doi.org/10.1021/acs.nanolett.0c01758
Nano Lett. 2020, 20, 5860−5865

artificially construct a sharp type-II interface in solid-state materials and hence to create a topological interface state in the experiment.[36,37] To overcome this difficulty, a new type-II interface designing strategy is developed, as shown in Figure 1.

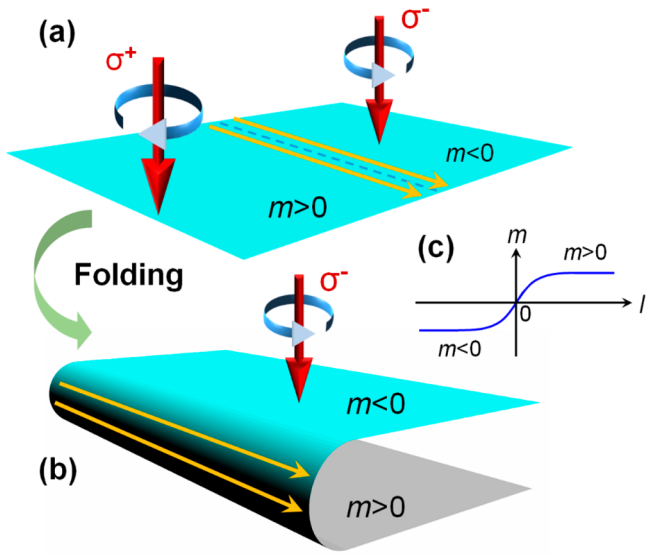

Figure 1. (a) Schematic graphene irradiated by two CPLs with opposite handedness. The light-induced mass term (m) changes sign across the boundary, creating two chiral-ISs localized at the interface region. (b) Schematic folded graphene irradiated by one CPL. The light-induced mass term changes sign from the top- to bottom-layer graphene, creating two chiral-ISs localized at the curved region. (c) Schematic mass-term inversion across the boundary (l = 0) for both panels a and b.

Since the sign of the light-induced mass term (m) in graphene is handedness-dependent,[13] in principle, one can construct a type-II interface by using two CPLs with different handedness,[17] as illustrated in Figure 1a. In the spinless model of graphene, each CPL will create a CI with a Chern number of C = 1 or −1. At the interface region, the edge state of two CIs join together and form two chiral-ISs, corresponding to a high-C CI with C = 2 or −2, as denoted by the two arrows. However, in practice, this two-light setup is too difficult to be realized in the experiment, because the light-irradiated area can hardly be controlled with nanoscale resolution, especially at the interface region between two beams of CPL.[17] Alternatively, however, we realized that, if graphene can be folded into the structure as shown in Figure 1b, a one-light setup is enough to construct a type-II interface in the curved region. Because top- and bottom-layer graphene will feel the effective light irradiation from opposite directions, becoming equivalent to the two-light setup. The light-induced mass-term inversion in the curved region is shown in Figure 1c, which can be exactly controlled by the folding process with atomic resolution. Consequently, such light-induced chiral-ISs can be detected more easily by current experimental techniques.[29]

In the following, we confirm the above proposal through numerical calculations. The tight-binding (TB) Hamiltonian of the folded graphene is constructed by an sp^3 model with both σ and π bands,[38] and light irradiation is described by the standard floquet band theory (see Supporting Information). To avoid the finite size effect, a semi-infinite structure is used in our model calculation.[39] In Figure 2a, graphene is folded along the armchair direction, forming a curved armchair-edge bilayer structure, which is semi-infinite along the y-direction and periodic along the x-direction. The gray-colored atoms

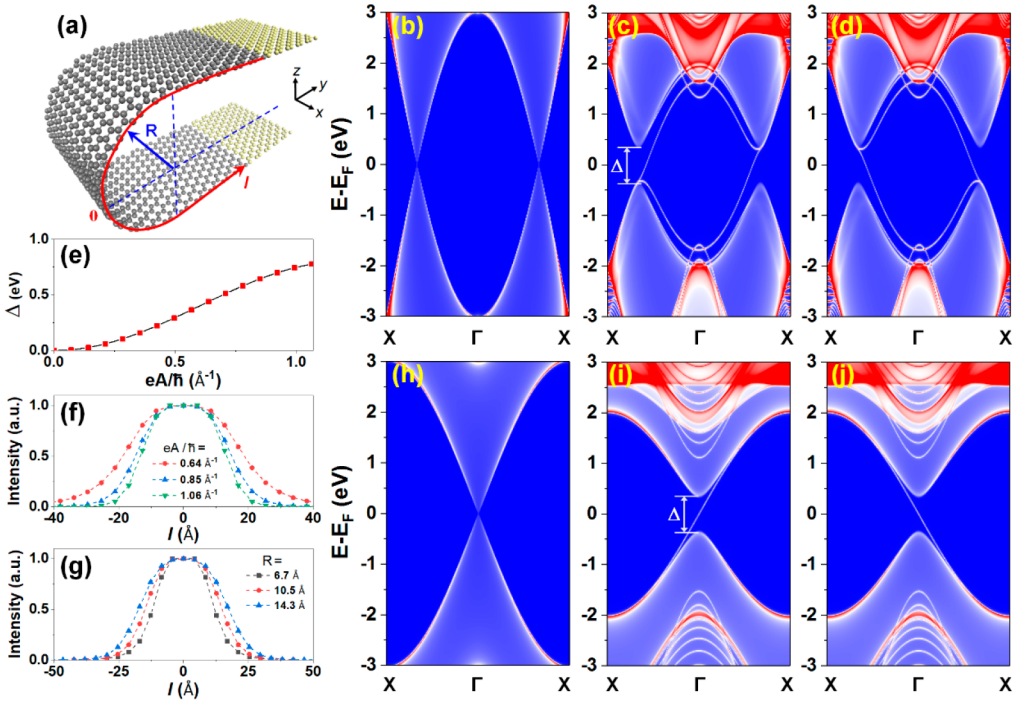

Figure 2. (a) Atomic structure of graphene folded along the armchair direction. (b) Spectral function of (a) without light irradiation. (c, d) Spectral function of (a) with left-handed and right-handed CPL irradiation. The light intensity is $eA/\hbar$ = 0.85 Å^{-1}. The red and blue color denotes the maximum and minimum value of spectral function, respectively. (e) Light-induced nontrivial band gap (Δ) vs light intensity. In panels b−e, l = 40 Å and R = 10.5 Å. (f, g) Spatial distribution of the chiral-IS vs light intensity with a fixed R = 10.5 Å and vs radius with a fixed $eA/\hbar$ = 0.85 Å^{-1}. Panels h−j are the same as panels b−d, but for graphene folded along the zigzag direction with l = 40 Å, R = 10.5 Å, and $eA/\hbar$ = 0.85 Å^{-1}.

https://dx.doi.org/10.1021/acs.nanolett.0c01758
Nano Lett. 2020, 20, 5860−5865

denote the curved region, characterized by the parameter of length l and curvature of radius R, while the green-colored atoms denote the flat semi-infinite region.

Without light irradiation, the typical band structure (the bright part in the spectral function) of graphene folded along the armchair direction is shown in Figure 2b. One can see a semimetal state with two Dirac points located at 2/3 along Γ-X direction. This band structure can be viewed as a combined band structure of one-half armchair SWCNT and two semi-infinite zigzag graphene nanoribbons. For both of them, the original Dirac points at K and K′ in graphene will be folded into the 2/3 location along Γ-X direction,[40,41] consistent with Figure 2b. Since they are connected together into a closed system without dangling bonds, the edge states of one-half armchair SWCNT and zigzag graphene nanoribbons are not present in the band structure. Additionally, the overall feature of such a band structure does not depend on the folding curvature of radius R (see Supporting Information).

Turning on light irradiation, the typical band structure with left-handed CPL is shown in Figure 2c. One notices that it has two striking features. First, the band degeneracy at both Dirac points is lifted, forming two gapped valleys. This is consistent with the light-induced nontrivial gap in graphene,[13] labeled as Δ. Second, there are two chiral-ISs in the band gap, connecting the valence and conduction band at both valleys with the same sign of group velocity continuously. This is consistent with the light-induced CI edge state in graphene.[13] Here, the two edge states indicate a Chern number of $C = 2$, that is, top- and bottom-layer graphene each contributes a chiral edge state with $C = 1$. Therefore, a high-C CI is realized in the folded graphene, directly confirming our proposal of a one-light setup. Moreover, the propagating direction of chiral-ISs can be easily tuned by the handedness of CPL. As shown in Figure 2d, the band structure with right-handed CPL is almost the same as that in Figure 2c, but the group velocity of both chiral-ISs changes the sign, indicating a Chern number of $C = -2$. The size of the nontrivial gap increases monotonically with the increasing intensity of CPL, as shown in Figure 2e. Meanwhile, there are always two chiral-ISs existing in the nontrivial gap, demonstrating the folded graphene an inherent CI.

To further identify these chiral-ISs, their spatial distribution at the Fermi-energy is also investigated. Here, the maximum intensity is rescaled to one for comparing the relative localization of different states. For a fixed R, the spatial distribution of chiral-IS with different light intensities is shown in Figure 2f. One can see that it exhibits an exponential decay from the apex of the curved region (coordinate origin of the red line in Figure 2a). Moreover, the chiral-IS decays faster with the increasing light intensity. On the other hand, for a fixed light intensity, the chiral-IS decays faster with the increasing curvature, as shown in Figure 2g. Consequently, the localization of chiral-IS can be efficiently tuned by both light intensity and folding curvature. The underlying physics of this phenomenon can be easily understood. The Hamiltonian of graphene with an inverted mass-term distribution along the y-direction (Figure 1c) can be written as $H(y) = \hbar v(k_x\sigma_x + k_y\sigma_y) + m(y)v^2\sigma_z$, where $m(y)$ is the mass term, and v is the group velocity. Its solution is $|\phi(y)|^2 \propto \exp(-\int_0^y[2|m(y')|v/\hbar]dy')$.[42] Clearly, it exponentially decays from the origin, and the decay rate is determined by the value of m. At a given position away from the origin, the above solution indicates that the chiral-IS decays faster with a larger value of the integral, that is, a larger m with a fast variation within the interface region. In the folded graphene, the largest value of m is determined by the light intensity, while the spatial variation of m is determined by the folding curvature (smaller R corresponds to a sharper m interface). Hence, this analysis is consistent with our numerical results.

In the experiment, graphene can be folded along different directions.[4] In order to identify the chirality dependence of our proposal, the band structure of graphene folded along the zigzag direction is also calculated. Without light irradiation, the two Dirac points in graphene are folded into the Γ point,[40,41] as shown in Figure 2h. With left-handed CPL irradiation, a nontrivial gap is opened at the Dirac point, and two degenerate chiral-ISs are created in the band gap, whose sign of group velocity is determined by the handedness of CPL, as shown in Figure 2i,j. All the key features are the same as those shown in Figure 2b–d. Therefore, the high-C CI in the folded graphene can be created independent of the folding direction, which significantly eases the experimental detection.

In the folded graphene, the chiral-ISs are localized at the curved region. This inspired us to further explore the limit of a seamlessly folded graphene structure, that is, the SWCNT. Without light irradiation, the metallic band structure of armchair SWCNT is shown in Figure 3a. With left-handed

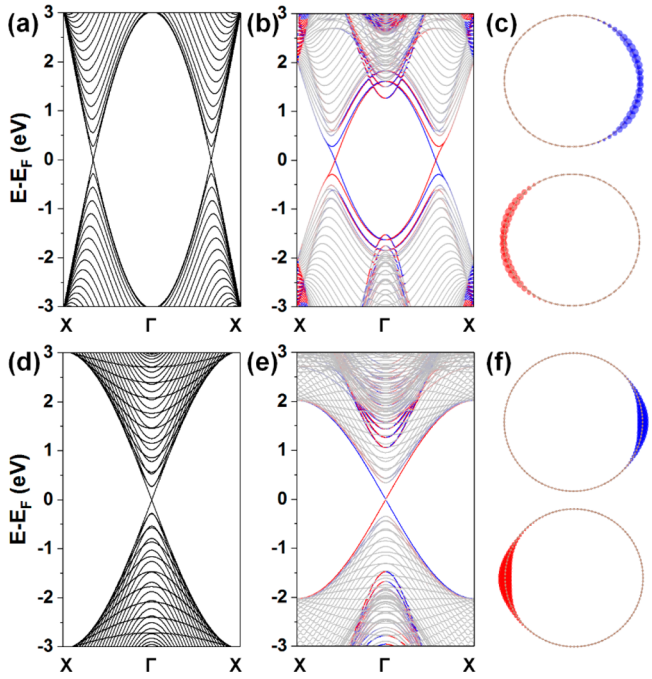

Figure 3. (a, d) Band structure of (34,34) armchair and (60,0) zigzag SWCNT. (b, e) Band structure of panels a and d with left-handed CPL irradiation. The light intensity is $eA/\hbar = 0.85$ Å^{-1}. The red and blue color denotes the weight of the wave function localized at the left- and right-half side, respectively. (c, f) Spatial distribution of the chiral-IS at the Fermi level in panels b and e.

CPL irradiation, two pairs of chiral-ISs appear in the band gap, as shown in Figure 3b. In each valley, there are two opposite prorogating chiral-ISs, crossing each other and forming a Dirac cone at the Fermi level. The red and blue color denotes the left- and right half-side localization of these chiral-ISs, which can be seen more clearly from a real-space plot at the Fermi energy, as shown in Figure 3c. Additionally, the prorogating direction of chiral-ISs can be inverted by changing the handedness of CPL. All these features are comparable to

https://dx.doi.org/10.1021/acs.nanolett.0c01758
Nano Lett. 2020, 20, 5860−5865

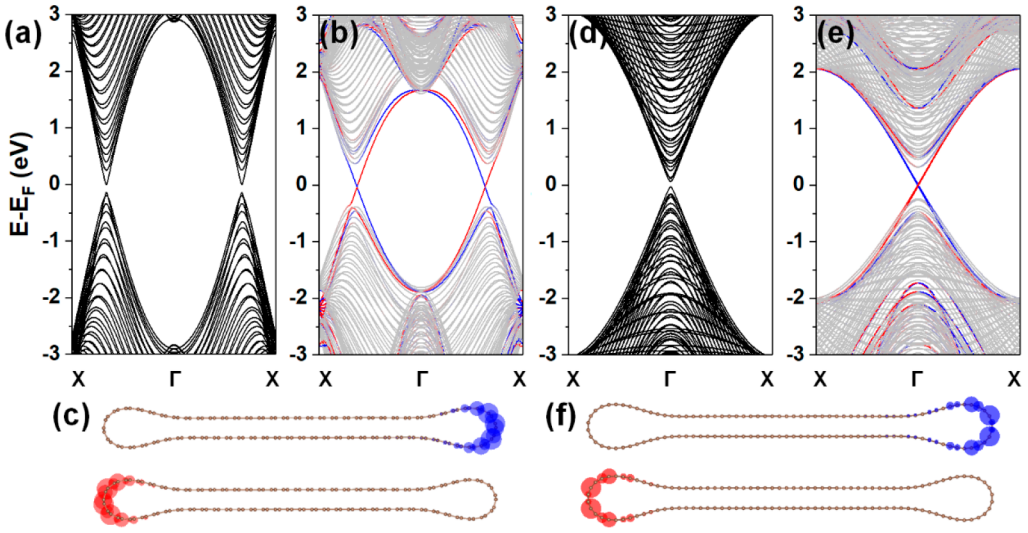

Figure 4. Panels a–c and d–f are the same as those shown in Figure 3, but for the collapsed (34,34) armchair and (60,0) zigzag SWCNT, respectively.

those shown in Figure 2b–d, demonstrating a light-induced CI with $C = 2$ in armchair SWCNT. Similar results for the zigzag SWCNT are shown in Figure 3d–f, which are comparable to those shown in Figure 2h–j. It is interesting to note that large SWCNTs are metastable, which may spontaneously collapse into a dogbone shape.[43] Thus, the collapsed structures of armchair and zigzag SWCNT are also investigated. Without light irradiation, besides the small gap opening at the Dirac point [Figure 4a,d], which is induced by interlayer coupling and symmetry breaking,[44] the overall band structure is similar to the circular SWCNT shown in Figure 3a,d. With left-handed CPL irradiation, two chiral-ISs within the band gap can be observed (Figure 4b,e), which are spatially localized at the left and right side of the collapsed SWCNT (Figure 4c,f), demonstrating a light-induced CI with $C = 2$. Therefore, this indicates that our proposal is valid not only for SWCNT of different chirality (folding direction) but also for a different size with a large tolerance of shape variation. Moreover, the similarity between the band structure of circular (Figure 3) and collapsed (Figure 4) SWCNT demonstrates that the interlayer interaction between top- and bottom-layer graphene has a tiny effect on the floquet band. This conclusion is also valid for the folded graphene shown in Figure 2 because of the large interlayer distance.

Since the folding structure of graphene can be precisely designed by using the recently developed STM technique,[4] it is possible to construct a more complex structure than what is shown in Figure 2a. Lastly, as an extension of our proposal, we have investigated a light-induced 3D CI in periodic folded graphene. It is well-known that 3D CI can be created by stacking 2D CI.[45,46] Beyond the designing strategy of the single folded graphene with one interface as discussed above, if graphene can be folded into a periodic structure with multi-interfaces, one may expect to develop a new method to make 3D CI. To confirm this idea, the band structure of periodic folded graphene along the armchair (Figure 5a) and zigzag (Figure 5c) direction with left-handed CPL irradiation is calculated, as shown in Figure 5b,d, respectively. One can see that the band structure looks rather similar to the SWCNT band along the Γ-X direction, but it is dispersionless along the Γ-Z direction (the stacking direction), showing the typical

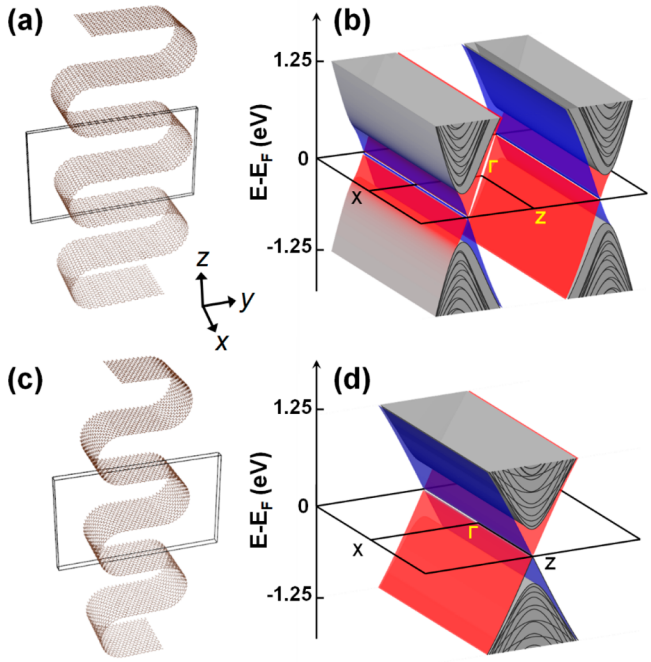

Figure 5. (a, c) Atomic structure of graphene periodic folded along the armchair and zigzag direction. The solid lines denote the unit cell of the folding structure, which is periodic along both x- and z-directions. (b, d) 3D band plotting of panels a and c with left-handed CPL irradiation. The other parameters are the same to those in Figure 2c,i. The red and blue colors have the same meaning as those in Figure 3.

band feature of 3D CI. The 3D Chern number can be calculated as $C^{3D} = \int_{-\pi/l_z}^{\pi/l_z}(C/2\pi)dk_z = C/l_z$,[46−48] where l_z is the unit-cell length along the z-direction, and $C = 2$ is the Chern number of single folded graphene. In this 3D CI, the conductance will be quantized in the unit of $2e^2/hl_z$. Therefore, different folding structures can be constructed to detect such a universal quantized conductance. Moreover, the nanorippled graphene with a periodic structure has already been

https://dx.doi.org/10.1021/acs.nanolett.0c01758
Nano Lett. 2020, 20, 5860−5865

synthesized in the experiment,[49,50] where a similar light-induced 3D CI is also identified (see Supporting Information).

Although the above results are calculated in the high-frequency region of CPL irradiation, we found that our proposed geometric engineering of CI is also realizable in the low-frequency region with multiband-crossings between floquet bands with a different floquet index (see Supporting Information), providing more convenience for the experimental detection. In conclusion, we propose an efficient one-light setup to inverse the nontrivial mass-term distribution in the folded graphene, realizing high-C and 3D CIs in single folded and periodic folded graphene, respectively. Moreover, the same physical principle can be applied to create high-C CI in SWCNT, independent of tube chirality (folding direction), size (radius), and shape variation (circular vs collapsed). Our results not only simplify the experimental setup to detect the light-induced chiral-IS in graphene but also open a new door to a priori designing topological state in 2D materials by a folding degree of freedom.

■ ASSOCIATED CONTENT

Supporting Information

The Supporting Information is available free of charge at https://pubs.acs.org/doi/xx https://pubs.acs.org/doi/10.1021/acs.nanolett.0c01758.

Chiral interface states of folded graphene vs radius R; chiral interface states of SWCNT vs tube size; 3D Chern insulator of nanorippled graphene; chiral interface states of SWCNT in low-frequency region; details of the calculation method (PDF)

■ AUTHOR INFORMATION

Corresponding Author

Zhengfei Wang − *Hefei National Laboratory for Physical Sciences at the Microscale, CAS Key Laboratory of Strongly-Coupled Quantum Matter Physics, University of Science and Technology of China, Hefei, Anhui 230026, China;* orcid.org/0000-0002-0788-9725; Email: zfwang15@ustc.edu.cn

Authors

Gan Zhao − *Hefei National Laboratory for Physical Sciences at the Microscale, CAS Key Laboratory of Strongly-Coupled Quantum Matter Physics, University of Science and Technology of China, Hefei, Anhui 230026, China*

Haimen Mu − *Hefei National Laboratory for Physical Sciences at the Microscale, CAS Key Laboratory of Strongly-Coupled Quantum Matter Physics, University of Science and Technology of China, Hefei, Anhui 230026, China*

Feng Liu − *Department of Materials Science and Engineering, University of Utah, Salt Lake City, Utah 84112, United States;* orcid.org/0000-0002-3701-8058

Complete contact information is available at: https://pubs.acs.org/10.1021/acs.nanolett.0c01758

Notes

The authors declare no competing financial interest.

■ ACKNOWLEDGMENTS

This work was supported by the NSFC (11774325 and 21603210), National Key Research and Development Program of China (2017YFA0204904), and Fundamental Research Funds for the Central Universities. F.L. was supported by DOE-BES (DE-FG02-04ER46148). We thank the Supercomputing Center at USTC for providing the computing resources.

■ REFERENCES

(1) Lu, W.; Lieber, C. M. Nanoelectronics from the bottom up. *Nat. Mater.* **2007**, *6*, 841−850.

(2) Žutić, I.; Fabian, J.; Das Sarma, S. Spintronics: Fundamentals and applications. *Rev. Mod. Phys.* **2004**, *76*, 323−410.

(3) Schaibley, J. R.; Yu, H.; Clark, G.; Rivera, P.; Ross, J. S.; Seyler, K. L.; Yao, W.; Xu, X. Valleytronics in 2D materials. *Nat. Rev. Mater.* **2016**, *1*, 16055.

(4) Chen, H.; Zhang, X. L.; Zhang, Y. Y.; Wang, D.; Bao, D.-L.; Que, Y.; Xiao, W.; Du, S.; Ouyang, M.; Pantelides, S. T.; Gao, H. J. Atomically precise, custom-design origami graphene nanostructures. *Science* **2019**, *365*, 1036−1040.

(5) Bistritzer, R.; MacDonald, A. H. Moiré bands in twisted double-layer graphene. *Proc. Natl. Acad. Sci. U. S. A.* **2011**, *108*, 12233−12237.

(6) Wang, Z. F.; Liu, F.; Chou, M. Y. Fractal Landau-level spectra in twisted bilayer graphene. *Nano Lett.* **2012**, *12*, 3833−3838.

(7) Cao, Y.; Fatemi, V.; Fang, S.; Watanabe, K.; Taniguchi, T.; Kaxiras, E.; Jarillo-Herrero, P. Unconventional superconductivity in magic-angle graphene superlattices. *Nature* **2018**, *556*, 43−50.

(8) Kerelsky, A.; McGilly, L. J.; Kennes, D. M.; Xian, L.; Yankowitz, M.; Chen, S.; Watanabe, K.; Taniguchi, T.; Hone, J.; Dean, C.; Rubio, A.; Pasupathy, A. N. Maximized electron interactions at the magic angle in twisted bilayer graphene. *Nature* **2019**, *572*, 95−100.

(9) Prada, E.; San-Jose, P.; Brey, L. Zero Landau level in folded graphene nanoribbons. *Phys. Rev. Lett.* **2010**, *105*, 106802.

(10) Kim, K.; Lee, Z.; Malone, B. D.; Chan, K. T.; Alemán, B.; Regan, W.; Gannett, W.; Crommie, M. F.; Cohen, M. L.; Zettl, A. Multiply folded graphene. *Phys. Rev. B: Condens. Matter Mater. Phys.* **2011**, *83*, 245433.

(11) Zhang, J.; Xiao, J.; Meng, X.; Monroe, C.; Huang, Y.; Zuo, J. M. Free folding of suspended graphene sheets by random mechanical stimulation. *Phys. Rev. Lett.* **2010**, *104*, 166805.

(12) Zhao, J.; Deng, Q.; Ly, T. H.; Han, G. H.; Sandeep, G.; Rümmeli, M. H. Two-dimensional membrane as elastic shell with proof on the folds revealed by three-dimensional atomic mapping. *Nat. Commun.* **2015**, *6*, 8935.

(13) Kitagawa, T.; Oka, T.; Brataas, A.; Fu, L.; Demler, E. Transport properties of nonequilibrium systems under the application of light: Photoinduced quantum Hall insulators without Landau levels. *Phys. Rev. B: Condens. Matter Mater. Phys.* **2011**, *84*, 235108.

(14) Lindner, N. H.; Refael, G.; Galitski, V. Floquet topological insulator in semiconductor quantum wells. *Nat. Phys.* **2011**, *7*, 490−495.

(15) Rechtsman, M. C.; Zeuner, J. M.; Plotnik, Y.; Lumer, Y.; Podolsky, D.; Dreisow, F.; Nolte, S.; Segev, M.; Szameit, A. Photonic Floquet topological insulators. *Nature* **2013**, *496*, 196−200.

(16) Rudner, M. S.; Lindner, N. H.; Berg, E.; Levin, M. Anomalous edge states and the bulk-edge correspondence for periodically driven two-dimensional systems. *Phys. Rev. X* **2013**, *3*, 031005.

(17) Calvo, H. L.; Foa Torres, L. E. F.; Perez-Piskunow, P. M.; Balseiro, C. A.; Usaj, G. Floquet interface states in illuminated three-dimensional topological insulators. *Phys. Rev. B: Condens. Matter Mater. Phys.* **2015**, *91*, No. 241404(R).

(18) Hübener, H.; Sentef, M. A.; Giovannini, U. D.; Kemper, A. F.; Rubio, A. Creating stable Floquet−Weyl semimetals by laser-driving of 3D Dirac materials. *Nat. Commun.* **2017**, *8*, 13940.

(19) Wang, Z. F.; Liu, Z.; Yang, J.; Liu, F. Light-induced type-II band inversion and quantum anomalous Hall state in monolayer FeSe. *Phys. Rev. Lett.* **2018**, *120*, 156406.

(20) Liu, H.; Sun, J. T.; Cheng, C.; Liu, F.; Meng, S. Photoinduced nonequilibrium topological states in strained black phosphorus. *Phys. Rev. Lett.* **2018**, *120*, 237403.

(21) Schuster, T.; Gazit, S.; Moore, J. E.; Yao, N. Y. Floquet Hopf insulators. *Phys. Rev. Lett.* **2019**, *123*, 266803.
(22) Peng, Y.; Refael, G. Floquet second-order topological insulators from nonsymmorphic space-time symmetries. *Phys. Rev. Lett.* **2019**, *123*, 016806.
(23) Li, X. S.; Wang, C.; Deng, M. X.; Duan, H. J.; Fu, P. H.; Wang, R. Q.; Sheng, L.; Xing, D. Y. Photon-induced Weyl half-metal phase and spin filter effect from topological Dirac semimetals. *Phys. Rev. Lett.* **2019**, *123*, 206601.
(24) Kane, C. L.; Mele, E. J. Quantum spin Hall effect in graphene. *Phys. Rev. Lett.* **2005**, *95*, 226801.
(25) Xiao, D.; Yao, W.; Niu, Q. Valley-contrasting physics in graphene: Magnetic moment and topological transport. *Phys. Rev. Lett.* **2007**, *99*, 236809.
(26) Qiao, Z.; Yang, S. A.; Feng, W.; Tse, W. K.; Ding, J.; Yao, Y.; Wang, J.; Niu, Q. Quantum anomalous Hall effect in graphene from Rashba and exchange effects. *Phys. Rev. B: Condens. Matter Mater. Phys.* **2010**, *82*, No. 161414(R).
(27) Liu, B.; Zhao, G.; Liu, Z.; Wang, Z. F. Two-dimensional quadrupole topological insulator in γ-graphyne. *Nano Lett.* **2019**, *19*, 6492.
(28) D'Alessio, L.; Rigol, M. Dynamical preparation of Floquet Chern insulators. *Nat. Commun.* **2015**, *6*, 8336.
(29) McIver, J. W.; Schulte, B.; Stein, F. U.; Matsuyama, T.; Jotzu, G.; Meier, G.; Cavalleri, A. Light-induced anomalous Hall effect in graphene. *Nat. Phys.* **2020**, *16*, 38−41.
(30) Hasan, M. Z.; Kane, C. L. Colloquium: Topological insulators. *Rev. Mod. Phys.* **2010**, *82*, 3045−3067.
(31) Yang, F.; Miao, L.; Wang, Z. F.; Yao, M. Y.; Zhu, F.; Song, Y. R.; Wang, M. X.; Xu, J. P.; Fedorov, A. V.; Sun, Z.; Zhang, G. B.; Liu, C.; Liu, F.; Qian, D.; Gao, C. L.; Jia, J. F. Spatial and energy distribution of topological edge states in single Bi(111) bilayer. *Phys. Rev. Lett.* **2012**, *109*, 016801.
(32) Reis, F.; Li, G.; Dudy, L.; Bauernfeind, M.; Glass, S.; Hanke, W.; Thomale, R.; Schäfer, J.; Claessen, R. Bismuthene on a SiC substrate: A candidate for a high-temperature quantum spin Hall material. *Science* **2017**, *357*, 287−290.
(33) Qiao, Z.; Jung, J.; Niu, Q.; MacDonald, A. H. Electronic highways in bilayer graphene. *Nano Lett.* **2011**, *11*, 3453−3459.
(34) Zhang, F.; MacDonald, A. H.; Mele, E. J. Valley Chern numbers and boundary modes in gapped bilayer graphene. *Proc. Natl. Acad. Sci. U. S. A.* **2013**, *110*, 10546−10551.
(35) Li, X.; Cao, T.; Niu, Q.; Shi, J.; Feng, J. Coupling the valley degree of freedom to antiferromagnetic order. *Proc. Natl. Acad. Sci. U. S. A.* **2013**, *110*, 3738−3742.
(36) Ju, L.; Shi, Z.; Nair, N.; Lv, Y.; Jin, C.; Velasco, J.; Ojeda-Aristizabal, C.; Bechtel, H. A.; Martin, M. C.; Zettl, A.; Analytis, J.; Wang, F. Topological valley transport at bilayer graphene domain walls. *Nature* **2015**, *520*, 650−655.
(37) Li, J.; Zhang, R. X.; Yin, Z.; Zhang, J.; Watanabe, K.; Taniguchi, T.; Liu, C.; Zhu, J. A valley valve and electron beam splitter. *Science* **2018**, *362*, 1149−1152.
(38) Hou, T.; Cheng, G.; Tse, W. K.; Zeng, C.; Qiao, Z. Topological zero-line modes in folded bilayer graphene. *Phys. Rev. B: Condens. Matter Mater. Phys.* **2018**, *98*, 245417.
(39) Huang, H.; Wang, Z.; Luo, N.; Liu, Z.; Lü, R.; Wu, J.; Duan, W. Time-reversal symmetry protected chiral interface states between quantum spin and quantum anomalous Hall insulators. *Phys. Rev. B: Condens. Matter Mater. Phys.* **2015**, *92*, 075138.
(40) Charlier, J. C.; Blase, X.; Roche, S. Electronic and transport properties of nanotubes. *Rev. Mod. Phys.* **2007**, *79*, 677−732.
(41) Castro Neto, A. H.; Guinea, F.; Peres, N. M. R.; Novoselov, K. S.; Geim, A. K. The electronic properties of graphene. *Rev. Mod. Phys.* **2009**, *81*, 109−162.
(42) Shen, S. Q. *Topological insulators: Dirac equation in condensed matters*; Springer, 2012.
(43) Xiao, J.; Liu, B.; Huang, Y.; Zuo, J.; Hwang, K. C.; Yu, M. F. Collapse and stability of single- and multi-wall carbon nanotubes. *Nanotechnology* **2007**, *18*, 395703.
(44) Lu, J. Q.; Wu, J.; Duan, W.; Liu, F.; Zhu, B. F.; Gu, B. L. Metal-to-semiconductor transition in squashed armchair carbon nanotubes. *Phys. Rev. Lett.* **2003**, *90*, 156601.
(45) Hughes, T. L.; Prodan, E.; Bernevig, B. A. Inversion-symmetric topological insulators. *Phys. Rev. B: Condens. Matter Mater. Phys.* **2011**, *83*, 245132.
(46) Jin, Y. J.; Wang, R.; Xia, B. W.; Zheng, B. B.; Xu, H. Three-dimensional quantum anomalous Hall effect in ferromagnetic insulators. *Phys. Rev. B: Condens. Matter Mater. Phys.* **2018**, *98*, No. 081101(R).
(47) Halperin, B. I. Possible states for a three-dimensional electron gas in a strong magnetic field. *Jpn. J. Appl. Phys. Suppl.* **1987**, *26*, 1913−1919.
(48) Kohmoto, M.; Halperin, B. I.; Wu, Y. S. Diophantine equation for the three-dimensional quantum Hall effect. *Phys. Rev. B: Condens. Matter Mater. Phys.* **1992**, *45*, 13488−13493.
(49) Bao, W.; Miao, F.; Chen, Z.; Zhang, H.; Jang, W.; Dames, C.; Lau, C. N. Controlled ripple texturing of suspended graphene and ultrathin graphite membranes. *Nat. Nanotechnol.* **2009**, *4*, 562−566.
(50) Deng, S.; Berry, V. Wrinkled, rippled and crumpled graphene: an overview of formation mechanism, electronic properties, and applications. *Mater. Today* **2016**, *19*, 197−212.

https://dx.doi.org/10.1021/acs.nanolett.0c01758
Nano Lett. 2020, 20, 5860−5865